UXO Classification

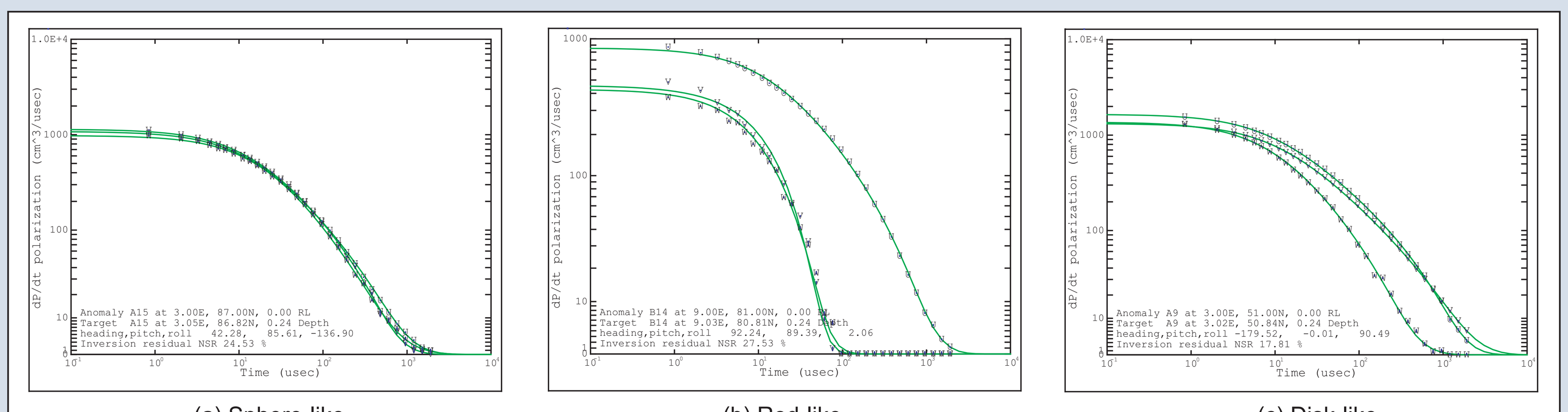

(a) Sphere-like (b) Rod-like (c) Disk-like

Target Polarizability Transients

Several typical target polarizability transients are shown above. If the target has spherical symmetry, like the sphere in the left panel (a), its polarizability response is the same along all three axes. Rod-like ferrous objects, middle panel (b), have the stronger polarizability along their longitudinal axis and two weaker but equal polarizability transients along their two tranverse axes. Disk-like ferrous objects, right panel (c) have weaker polarizability along their longitudinal axes and two stronger and nearly equal polarizability responses along their two tranverse axes.

Modeling and Classification

The data processing and modeling flow for static follow-up TEM measurements is shown in the block diagram at right. Follow-up measurements revisit target anomalies picked from the results of a dynamic TEM survey. For each target listed on the follow-up dig sheet, careful static TEM measurements are made over a small patch overlying the target anomaly. The patch of multi-component TEM transients are inverted to three polarizability transients, one along each axis of the target model. Model parameters are used to classify the target model into uxo or clutter categories.

We are currently developing and testing two different classification algorithms. The algorithms are ultimately based on the numerous model parameters that are returned from our TEM inversion program, DNTdipole.

1. MDA (Multiple Discriminant Analysis), based on multivariate statistics.
2. ANN (Artificial Neural Network), based on knowledge-based neural networks.

Modeling and Classification Data Flow

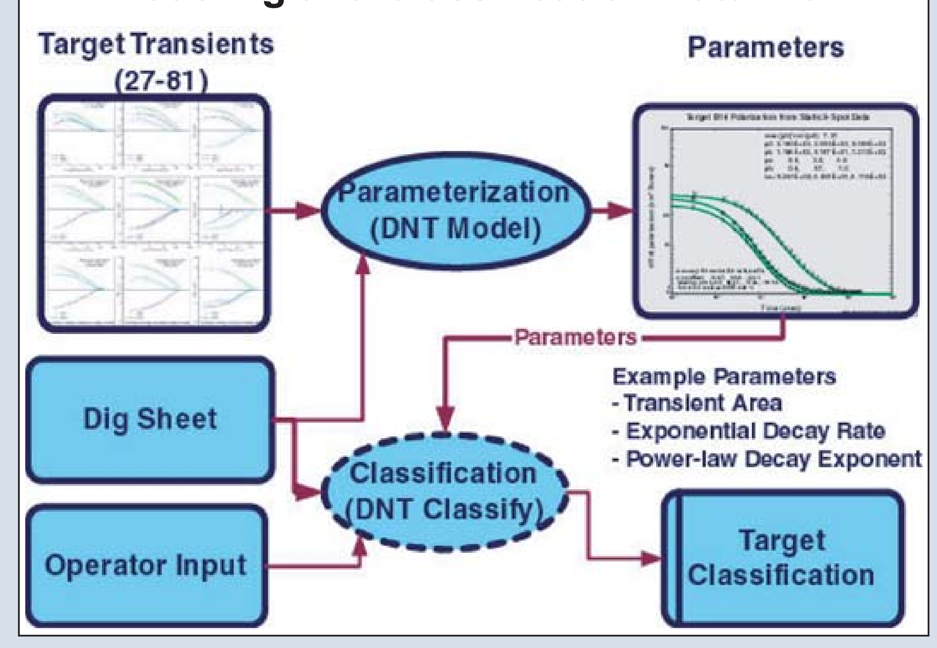

MDA Classification

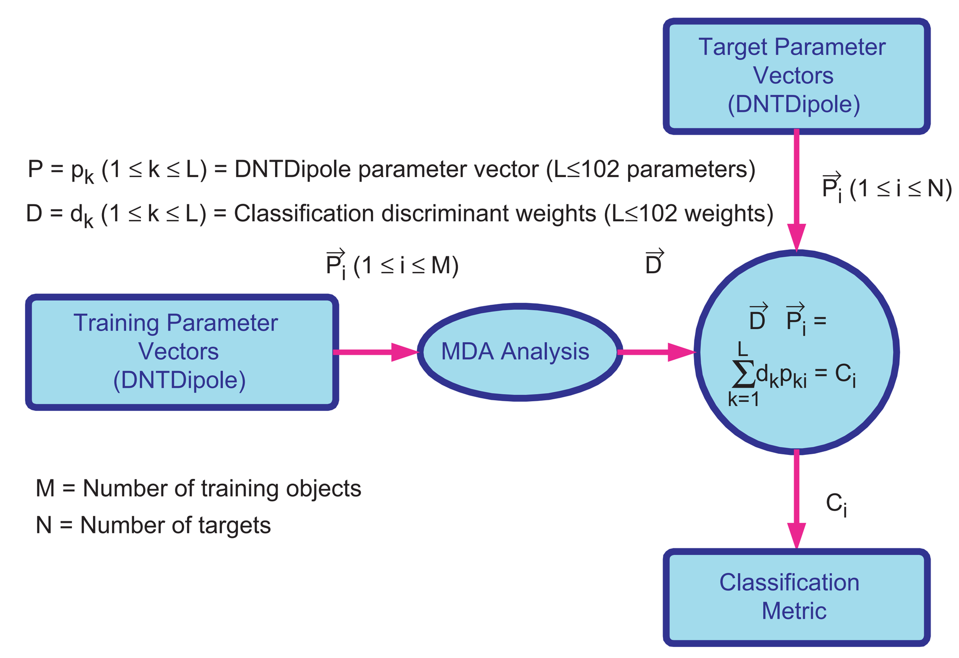

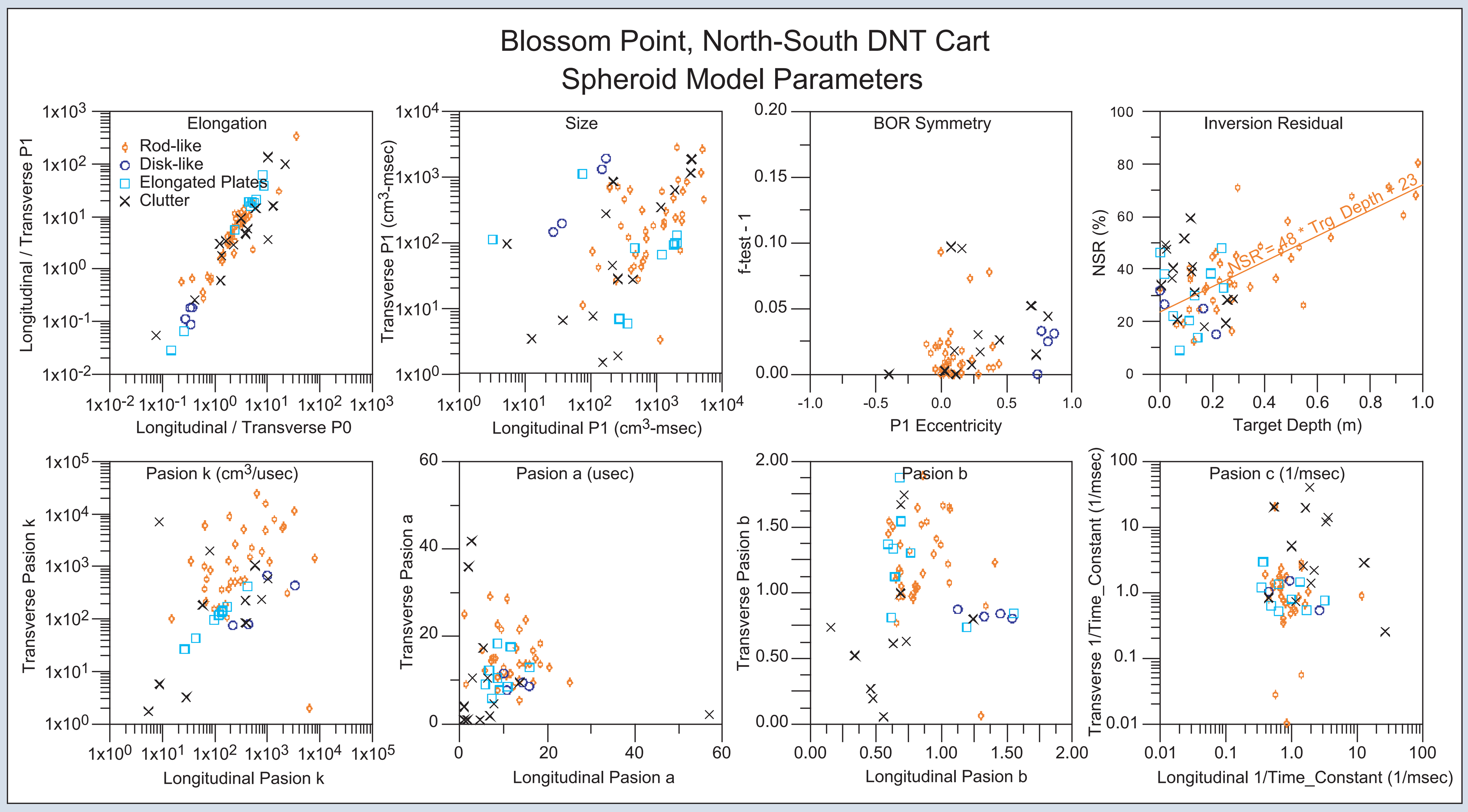

Model Parameter Scatter Plots, Blossom Point Data

Above are model parameter scatter plots created using inversion results of Blossom Point North-South DNT Cart data with the target model fixed at known location and orientation. A set of 8 scatter plots is shown for a set of 73 Blossom Point targets. To help show the separation of various target classes in the plots, we have divided the targets into four groups: rods, spheres, disks, and irregular clutter. The 8 plots correspond to 8 sets of model parameters from polarizability transient amplitude and shape. The top row of plot panels depicts model parameters related to target size, shape, symmetry and depth. The bottom row of plot panels shows all of the Pasion model parameters for longitudinal and transverse polarizability, summarizing the polarizability transient shape. Individual combinations of model parameters are related to target attributes useful for categorization.

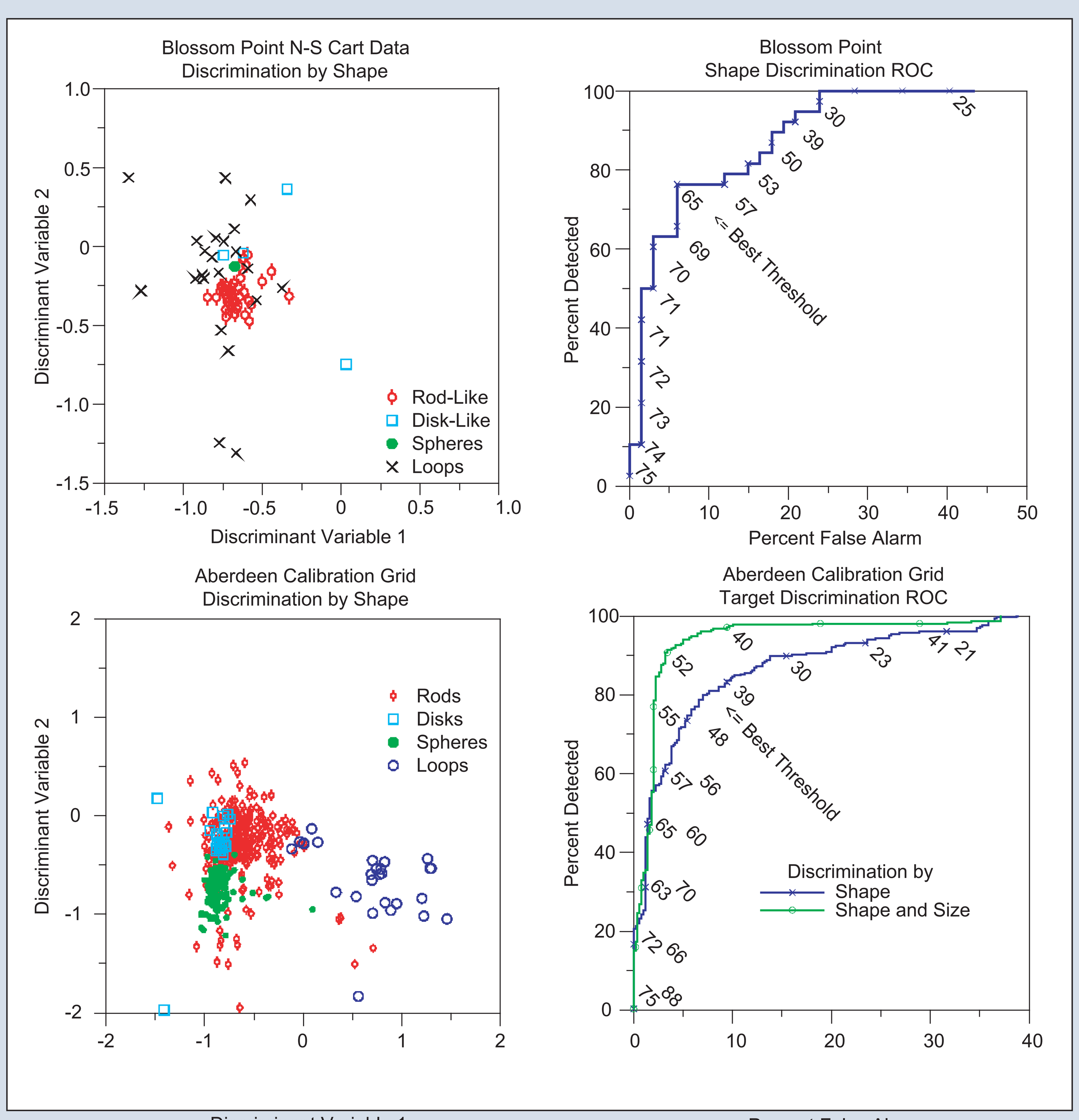

Shape-based Discrimination Results

A set of four plots are shown above; the upper two plots are from Blossom Point data, and the lower two are from Aberdeen Test Center data. These plots illustrate the separation of targets using shape-based discrimination parameters. Since most UXO are ferrous and have an elongated shape with cylindrical symmetry, classification by shape provides a useful tool for target discrimination. We used model parameter estimates from inversion of Blossom Point and Aberdeen calibration grid data to construct a shape-based ranking metric.

The left panels show the separation of Blossom Point or Aberdeen target data into groups based on statistically-based shape discrimination variables. These scatter plots exhibit good separation between rod-like objects and clutter. Many of the elongated plates get classified as the rod-like targets and labeled as uxo rather than being discriminated as non-uxo. The right panels above are the resulting shape-based discrimination ROC curves for the Blossom Point North-South DNT Cart data (top right panel) and the Aberdeen Calibration grid DNT Cart data (bottom right panel).

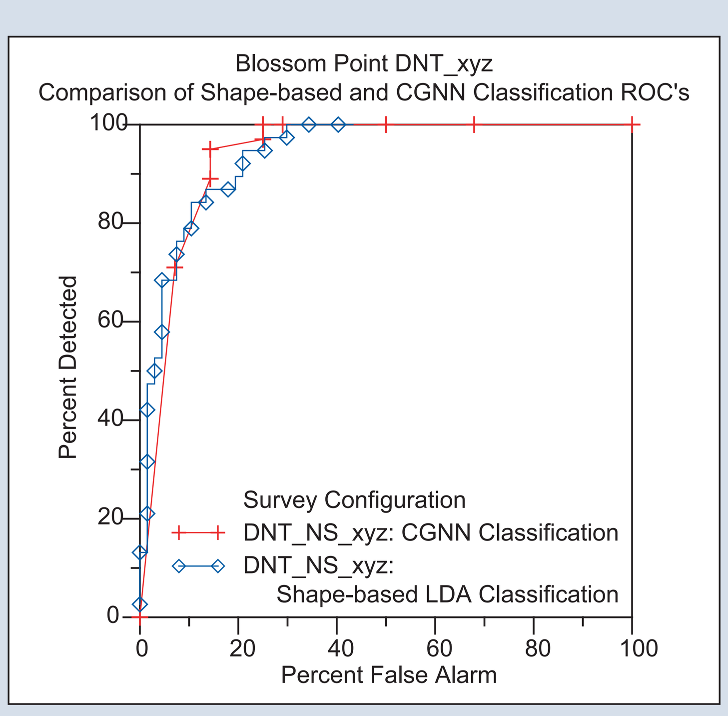

ANN Classification

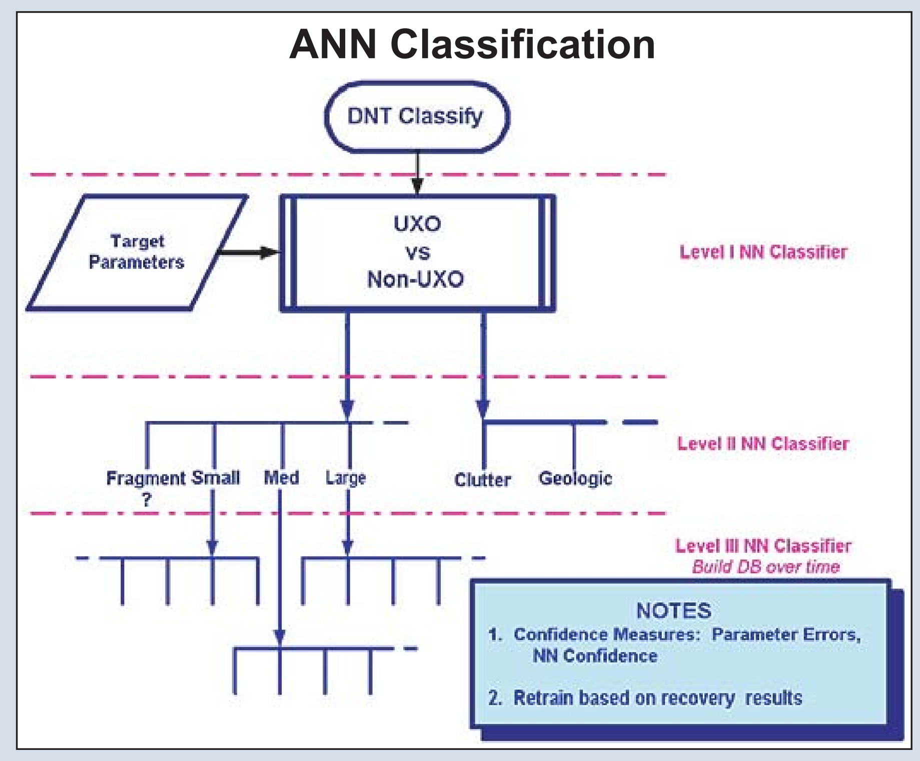

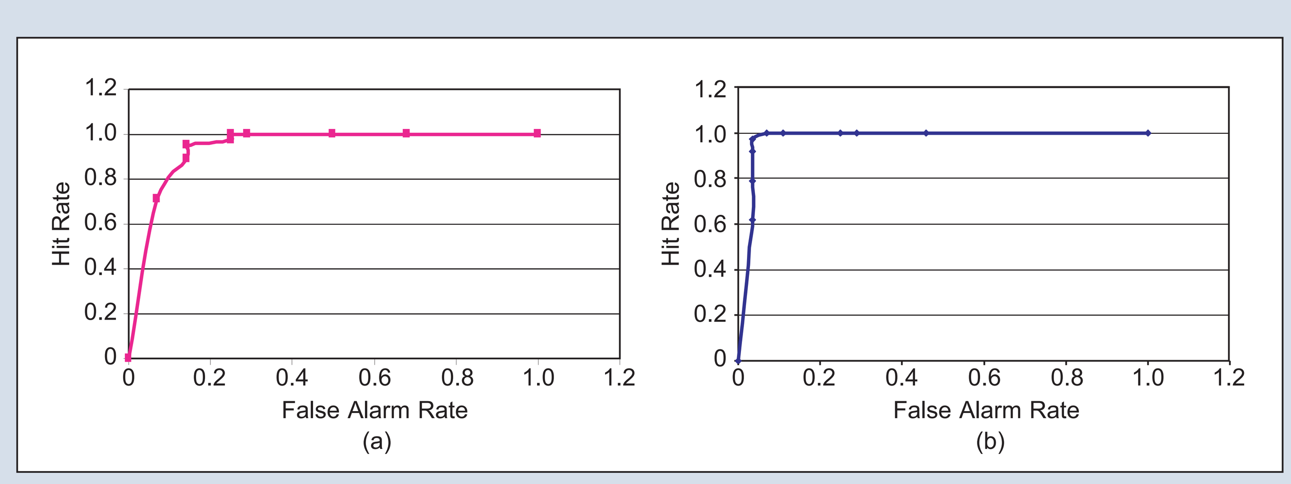

Target Classification Using Artificial Neural Networks (ANNs)

We used a multi-layer perceptron architecture with a combination of backpropagation and conjugate gradient learning. The network architecture consisted of 14 model-parameter inputs, 7 hidden units, and 1 output (1=uxo, 0=clutter).

The two discrimination ROC curves above are from neural network classification. First we used 55 model parameter sets from inversion of Blossom Point North-South DNT Cart data, 36 parameters sets from the Ajo Road test site near Tucson, and modeling results from static Helmholtz coil testing. The left panel, (a), shows discrimination results as the decision threshold is varied from 0 to 1. For a second CG network, we used 55 model parameters sets from Blossom Point for training and 12 for testing. No measurements from other surveys were used for testing. The ROC curve for this network is shown in right panel, (b), above.

Discrimination results are significantly improved when model parameters are derived from TEM measurements with similar acquisition characteristics. Good discrimination weighting is dependent upon consistent model parameter statistics and those statistics change when the TEM data acquisition characteristics such as Tx turn-off ramp length or transient delay time windows are different.